

# Uncertainty assessment of future projections on water resources according to climate downscaling and hydrological models

Moon-Hwan Lee and Deg-Hyo Bae

## ABSTRACT

Quantifying the uncertainty of future projection is important to assess the reliable climate change impact. In this sense, this study is aimed at investigating the uncertainty sources of various water variables (seasonal dam inflow, 1-day maximum dam inflow, and 30-day minimum dam inflow) according to downscaling methods and hydrological modeling. Five regional climate models (RCMs), five statistical post-processing methods and two hydrological models were applied for the uncertainty analysis. The changes for seasonal dam inflow are 0.1, 58.8, 5.1, and 1.1 mm for the SWAT model and 2.1, 76.1, -8.5, and -2.9 mm for the VIC model in spring, summer, autumn, and winter, respectively. The effects of the hydrological model is smaller than that of RCM for future projections of the seasonal dam inflow. The changes of annual 1-day maximum dam inflow vary according to the selection of RCM whereas the changes of annual 30-day minimum dam inflow are sensitive to the selection of hydrological model. The RCM is the dominant source of uncertainty of all seasonal dam inflow (except for winter) and high flow, whereas the hydrological model is the dominant source of uncertainty in winter dam inflow and low flow. Considering these results, the appropriate multi-model ensemble chain according to target variable will be necessary for reliable climate change impact assessment.

**Key words** | climate change, hydrological model, uncertainty analysis, variance analysis, water resources

**Moon-Hwan Lee**  
**Deg-Hyo Bae** (corresponding author)  
Department of Civil and Environmental  
Engineering,  
Sejong University,  
Seoul 05006,  
Korea  
E-mail: [dhbae@sejong.ac.kr](mailto:dhbae@sejong.ac.kr)

## INTRODUCTION

Several studies have shown that the risk of water disasters, such as flood, drought, and water shortage, will be exacerbated due to climate change (IPCC 2013; Raghavan *et al.* 2014; Yu *et al.* 2014; Lee & Bae 2015). Therefore, it is necessary to consider the climate change impact assessment on water resource management plan. For this, the results of climate change impact assessment should have high reliability. However, these results have many uncertainties caused by several sources such as greenhouse gas emission scenario, global climate simulation, regional climate simulation, and hydrological modeling (Bae *et al.* 2011). In other words, the

projection results are different depending on which methods or models are applied. Understanding and quantifying these uncertainties are important to assess the reliable climate change impact (Mani & Tsai 2017). The development of a methodology to evaluate the uncertainties quantitatively is required because the uncertainty analysis can be applied to performance metrics of direct interest to stakeholders (Harvey *et al.* 2012).

Numerous studies have used multi-model ensembles to investigate climate change impact and the associated uncertainty on future runoff (Wilby & Harris 2006; Kay *et al.*

2009; Bae *et al.* 2011; Chen *et al.* 2011; Xu *et al.* 2011; Teng *et al.* 2012; Jung *et al.* 2013). Wilby & Harris (2006) showed that the cumulative distribution functions of low flows were more sensitive to the choice of global climate models (GCMs) and downscaling methods than the selection of hydrologic models or emission scenario. Kay *et al.* (2009) suggested that GCM is a dominant uncertainty source when the changes in flood frequency were assessed for a future period in England. Xu *et al.* (2011) evaluated the uncertainty of high and low flow according to the selection of GCM and scenario. Chen *et al.* (2011) assessed the stream flows using two emission scenarios, six GCMs, four downscaling methods, and three hydrological models. Their results showed that the uncertainty of GCM is higher than the other steps. Bae *et al.* (2011) showed that the uncertainties from GCM and hydrological models are more significant in the dry season than in the wet season, and also uncertainty from GCM was shown to be more significant than that from the hydrological model. Zhang *et al.* (2014) evaluated the impacts of climate change on diversion strategies for a water deficit reservoir using the predicted runoff based on an ensemble of three GCMs under three climate scenarios.

Previous studies focused on the range estimation of projection results using ensemble models and uncertainty analysis were carried out by using the simple comparison of result range for each step. Recently, few studies have proposed methodologies for quantifying the uncertainty in climate change impact assessments. Deque *et al.* (2007) assessed the uncertainties in the model projection of regional climate simulations for Europe and developed a variance decomposition method to assess the uncertainties due to different emission scenarios, GCMs, and regional climate models (RCMs). Bosshard *et al.* (2013) presented a methodology to separate the uncertainties arising from the climate model, statistical post-processing scheme, and hydrological model. This methodology can quantitatively decompose the total ensemble uncertainty into contributions from an individual ensemble source. Therefore, this study is aimed at investigating the uncertainty sources from downscaling methods (regional climate modeling, statistical post-processing), hydrological model, and to assess the various water variables such as seasonal dam inflow and annual 1-day maximum dam inflow, annual 30-day minimum dam inflow to investigate the cause of uncertainty according to the water resources variables.

## METHODOLOGY

### Climate change scenario

The global climate change scenarios that are produced by the GCM with emission scenarios were used for assessing the impact of climate change on water resources (Bae *et al.* 2008). A downscaling method is necessary to improve the resolution of the global climate change scenarios to local scale which is appropriate for the basin scale. The dynamic downscaling method produces high-resolution climate information by using a RCM with the climate data simulated by GCM as boundary conditions.

To assess the uncertainties from downscaling methods, the results of the CORDEX (COordinated Regional climate Downscaling EXperiment) East Asia project were used in this study. The major aims of the CORDEX are to provide a coordinated model evaluation framework, a climate projection framework, and an interface to the applicants of the climate simulations in climate change impact, adaptation, and mitigation studies. CORDEX-East Asia is the East-Asian branch of the CORDEX and they have produced the ensemble climate simulations based on multiple dynamical downscaling models driven by a global climate model. The climate change scenarios were simulated by five RCMs (HadGEM3-RA, RegCM4, SNU-MM5, SNU-WRF, and YSU-RSM) driven by HadGEM2-AO (Atmosphere-Ocean coupled Hadley center Global Environmental Model version 2) of the National Institute of Meteorological Research (NIMR) (Baek *et al.* 2013).

The five RCMs can be divided into three non-hydrostatic (HadGEM3-RA, SNU-MM5, and SNU-WRF) and two hydrostatic RCMs (RegCM4 and YSU-RSM). The horizontal resolution is 50 km (0.44° for HadGEM3-RA). Different physical schemes including convection, land surface, planetary boundary layer, and radiation are applied across RCMs as summarized in Table 2 of Park *et al.* (2016). Further details of models configuration are referred to Suh *et al.* (2012) and Park *et al.* (2016).

### Statistical post-processing method

There are biases in the climate simulation data produced by climate models due to the limitation of model structure and

parameterization. Therefore, the statistical post-processing method is necessary to use climate simulation data. For this study, we used the linear scaling method (LS), variance scaling method (VS), quantile mapping method (QM), change factor method (CF), and step-wise scaling method (SWS). Because these five methods are common and popular methodologies for bias correction, we briefly describe the basic concepts of these methods in this manuscript. More detailed descriptions can be found in [Chen \*et al.\* \(2011\)](#), [Teutschbein & Seibert \(2012\)](#), [Lee & Bae \(2015\)](#), and [Lee & Bae \(2013\)](#).

The LS method is the most commonly used for climate change impact studies. This method uses differences of monthly average between observation and scenario ([Chen \*et al.\* 2011](#)). The VS method is the method using differences of monthly mean and standard deviation between observation and scenario ([Teutschbein & Seibert 2012](#)). QM is a method to correct the distribution function of simulated climate values corresponding to the observed distribution function of daily climate data ([Teutschbein & Seibert 2012](#)). The CF method is to determine monthly change ratio between present and future climate simulation and then multiply the ratio to the past historical climate data ([Lee & Bae 2015](#)). The SWS method is divided into three categories (extreme event, dry event, and the others). The extreme events, wet-dry days and the others are corrected by using the regression method, quantile mapping method, and mean and variance scaling method ([Lee & Bae 2013](#)).

### Hydrological model

A semi-distributed hydrological model, SWAT (Soil and Water Assessment Tool), and distributed model, VIC, were used for simulating the dam inflow. The SWAT model was developed by the Agricultural Research Service in USDA and has been widely applied to predict the effects of climate and vegetative changes, groundwater withdrawals and reservoir management ([Arnold \*et al.\* 1993](#)). The VIC model developed by Dr Dennis Lettenmaier research group at the University of Washington is used for the analysis of water availability over the Asian Monsoon region ([Liang \*et al.\* 1994](#)). It shares several basic features with other land surface models that are commonly coupled to global circulation models. The key characteristics of the grid-based VIC are

the representation of vegetation heterogeneity, multiple soil layers with variable infiltration, and non-linear base flow. The land surface is modeled as a grid of large (>1 km), flat, uniform cells. Sub-grid heterogeneity is handled via statistical distributions. Inputs are time series of daily or sub-daily meteorological drivers. Land-atmosphere fluxes and the water and energy balances at the land surface are simulated at a daily or sub-daily time step.

### Uncertainty assessment method

There are several uncertainties assessment methods such as Bayesian Model Average ([Steinschneider \*et al.\* 2012](#)), GLUE ([Bastola \*et al.\* 2012](#)), Paired t-test ([Chen \*et al.\* 2011](#)), Monte-Carlo simulation ([Wilby & Harris 2006](#)), Multi-objective optimization function ([Vojinovic \*et al.\* 2014](#)) and Variance analysis ([Bosshard \*et al.\* 2013](#)). This study focused on quantification of the uncertainty contribution for each step, so this study used the variance analysis. For this study, the uncertainty sources consist of a regional climate model (hereafter referred to as RCM), statistical post-processing (hereafter referred to as SPP), and a hydrological model (hereafter referred to as HYM). The total uncertainty defined in this study is the variance of the changes ( $U_{FUT}$ ) in future dam inflow ( $Q_{FUT}$ ) relative to the historical dam inflow ( $Q_{CTL}$ ) (Equation (1)):

$$U_{FUT} = Q_{FUT} - Q_{CTL} \quad (1)$$

The five RCMs (HadGEM3-RA, RegCM4, MM5, WRF, and RSM), five SPPs (LS, VS, QM, CF, and SWS) and two HYMs (SWAT, VIC) were applied, and the total 50 ensemble members ( $5 \times 5 \times 2$ ) were generated. In this case, the number of HYMs is lower than the other steps. This leads to some errors according to different sample sizes because variance analysis is based on variance concept. So, this study applied the sub-sampling method. We selected two RCMs and two SPPs in 25 possible RCM and SPP pairs in each sub-sampling iteration ([Figure 1](#)). Therefore, each experiment consists of two RCMs  $\times$  two SPPs  $\times$  two HYMs, and the numbers of total iteration are 100 times.

The total variance can be calculated as Equation (2) considering sub-sampling. The sum of squares for each

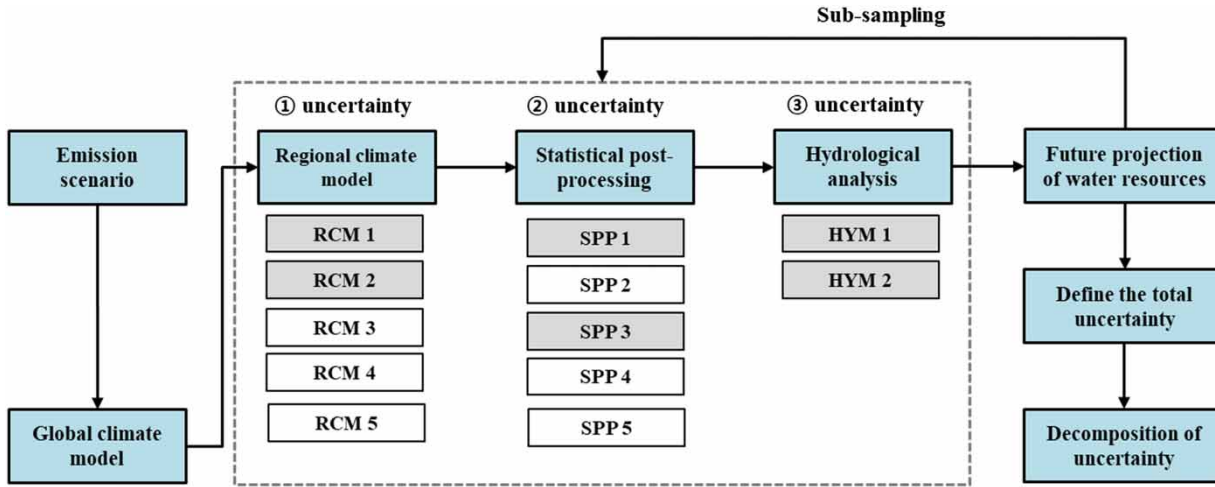


Figure 1 | Modeling framework for uncertainty assessment using variance analysis with sub-sampling method.

effect can be estimated as Equations (3)–(5). In this study, the interaction effects can be calculated as Equation (6):

$$SS_{total} = \frac{1}{I} \sum_{i=1}^I \left[ \sum_{ir=1}^2 \sum_{is=1}^2 \sum_{ih=1}^2 (U_{i,ir,is,ih} - U_{i,*,*,*})^2 \right] \quad (2)$$

$$SS_{RCM} = \frac{1}{I} \sum_{i=1}^I \left[ 2 \times 2 \times \sum_{ir=1}^2 (U_{i,ir,*,*} - U_{i,*,*,*})^2 \right] \quad (3)$$

$$SS_{RCM,SPP} = \frac{1}{I} \sum_{i=1}^I \left[ 2 \times \sum_{ir=1}^2 \sum_{is=1}^2 (U_{i,ir,is,*} - U_{i,ir,*,*} - U_{i,*,is,*} + U_{i,*,*,*})^2 \right] \quad (4)$$

$$SS_{RCM,SPP,HYM} = \frac{1}{I} \sum_{i=1}^I \left[ \sum_{ir=1}^2 \sum_{is=1}^2 \sum_{ih=1}^2 (U_{i,ir,is,ih} - U_{i,ir,is,*} - U_{i,ir,*,ih} - U_{i,*,is,ih} + U_{i,ir,*,*} + U_{i,*,is,*} + U_{i,*,*,ih} - U_{i,*,*,*})^2 \right] \quad (5)$$

$$SS_{INT} = SS_{RCM,SPP} + SS_{RCM,HYM} + SS_{SPP,HYM} + SS_{RCM,SPP,HYM}, \quad (6)$$

where  $i$  is iteration for sub-sampling,  $ir, is, ih$  indicate a specific RCM, SPP, and HYM, respectively. \* indicates average value.  $U_{i,ir,is,ih}$  is a change in dam inflow between

historical and future periods at specific RCM, SPP, and HYM.  $U_{i,*,*,*}$  is average change in dam inflow of two RCMs, two SPPs, and two HYMs for certain iteration ( $i$ ).  $U_{i,ir,*,ih}$  is average change in the dam inflow of two SPPs at specific RCM and HYM for certain iteration ( $i$ ).  $I$  is the number of total iterations at 100 times.

Each contribution ( $\eta^2$ ) can be estimated as below (Equations (7)–(9)). The contribution has a value of 0 to 1:

$$\eta_{RCM}^2 = \frac{SS_{RCM}}{SS_{total}} \quad (7)$$

$$\eta_{RCM,SPP}^2 = \frac{SS_{RCM,SPP}}{SS_{total}} \quad (8)$$

$$\eta_{RCM,SPP,HYM}^2 = \frac{SS_{RCM,SPP,HYM}}{SS_{total}} \quad (9)$$

## STUDY AREA AND DATA COLLECTION

The study area is the Chungju-dam basin which is the uppermost basin in Han-river, South Korea (Figure 2). The blue line indicates the tributaries of the river in Chungju basin, and the black square indicates the location of the Chungju multi-purpose dam. This basin area is about 6,648 km<sup>2</sup>, elevation is about 70–1,569 m, and it is also a mountainous area of which approximately 82% is made up of forests. The

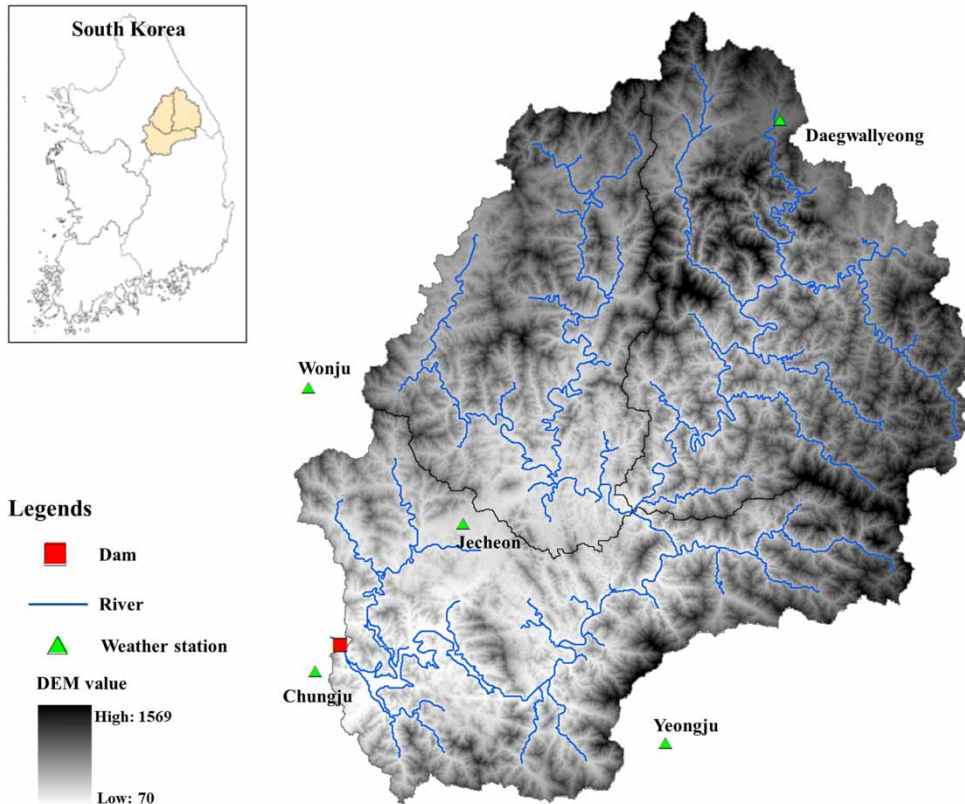


**Figure 2** | Study area in Chungju Basin, South Korea. Please refer to the online version of this paper to see this figure in colour: <http://dx.doi.org/10.2166/hydro.2018.132>.

Chungju dam is a very important multi-purpose dam that provides water supply (agricultural, industrial, living water) and flood control. The average dam inflow is about  $154.6 \text{ m}^3/\text{s}$ , the effective storage capacity is about 1,789 million  $\text{m}^3$  and the designed annual water supply capacity is about 3,380 million  $\text{m}^3$ .

High quality long-term climate and precipitation data are necessary for performing the hydrological simulation. There are various weather and rainfall stations in Chungju basin; this study used five KMA (Korea Meteorological Administration) weather stations and MOLIT (Ministry of Land, Infrastructure and Transport) rainfall stations which had been collecting data since 1981. For running the SWAT and VIC model, daily precipitation, maximum and minimum temperature, relative humidity, wind speed, solar radiation data are necessary. This study used five weather stations (Jecheon, Chungju, Wonju, Yeongju, and Dagwallyeong). The  $30 \times 30 \text{ m}$  digital elevation model of National Geographic Information Institute, land use of WAMIS, and detailed soil map of National Institute of Agricultural

Sciences were collected. CORDEX East Asia provided the dynamic downscaled climate change scenario. At this time, this project provides the HadGEM3-RA of NIMR, RegCM4 of Kongju National University, MM5, WRF of Seoul National University, and RSM of Yonsei University. The daily precipitation and daily maximum and minimum temperature were collected, and the data period is 1981–2005 for the historical period and 2011–2035 for a future period with RCP4.5.

## RESULTS AND ANALYSIS

### Calibration of hydrological model

This study used two hydrological models: SWAT (Bae *et al.* 2011) and VIC (Bae *et al.* 2017). The SWAT model was calibrated with observed flow data from 1996–2005 and verified with data from 1986–1995 at Chungju Basin, described by Bae *et al.* (2011). We also draw here on VIC model results



from the 1/8 degree implementation for South Korea, described by Bae *et al.* (2017). The VIC model was set up over South Korea with a spatial resolution of 1/8° (approximately 12.5 km) and they estimated the LSM parameters using observed runoff data from 1981 to 2004. Therefore, this study only assessed the performances of two models during 2001–2005. Statistical assessments such as correlation coefficient (CC), root mean square error (RMSE), model efficiency (ME), and volume error (VE) were performed (Table 1). The results of SWAT and VIC model are approximately 0.89, 0.83 (CC), 3.05, 3.90 (RMSE), 0.80, 0.69 (ME), –0.1, 3.3% (VE), respectively. These results show that the performance of the model is quite satisfactory for analyzing the dam inflow data. In addition, the simulated and observed dam inflows were analyzed for assessing the trend of high and low flow from 2001 to 2005 (Figure 3). The simulated dam inflow at the outlet of this study area was in good agreement with the observed dam inflow.

The annual 1-day maximum dam inflow (hereafter referred to as MXDI01) and 30-day minimum dam inflow (hereafter referred to as MNDI30) are used to evaluate the high and low flow simulation capability. The mean, standard deviation, maximum and minimum value are summarized in Table 2. For the MXDI01, the average of observed data is about 72.6 mm, standard deviation is 43.3 mm, maximum is 170.8 mm, and minimum is 19.5 mm. As can be seen in Table 2, the SWAT model estimated the mean and standard deviation are lower than those of observation, while maximum and minimum values are almost similar to those of observation. However, the VIC model estimated that the mean value is lower and the standard deviation is higher than those of observation. As regards to the MNDI30, the average is about 6.5 mm, standard deviation is 2.2 mm,

maximum is 11.3 mm, and minimum is 3.5 mm. The MNDI30 of SWAT is similar for all statistics of observed data but the VIC model simulated larger than observed data. These results showed that the accuracy of the SWAT model is higher than that of the VIC model for MXDI01 and MNDI30 in this study area.

### Biases in historical dam inflow simulation

Because climate change scenarios have some biases, this study applied the five SPP methods (LS, VS, QM, CF, and SWS) presented above under ‘Statistical post-processing method’. This study performed hydrological simulations using the bias-corrected climate change scenarios, a total of 50 hydrological simulations were generated for the historical period (5 × 5 × 2). Table 3 shows the average value of biases and volume errors of seasonal dam inflow, MXDI01, MNDI30. The biases (volume errors) of seasonal dam inflow are underestimated by 11.6 mm (8.5%), 10.9 mm (7.9%), 5.6 mm (4.1%), 4.2 mm (3.1%) for spring, and 24.3 mm (5.0%), 15.7 mm (3.2%), 11.4 mm (2.3%), 9.3 mm (1.9%) for summer, and –7.7 mm (–3.5%), –8.4 mm (–3.8%), 5.1 mm (2.3%), –0.5 mm (–0.2%) for autumn, and –0.4 mm (–0.8%), –1.8 mm (–3.5%), 3.0 mm (5.8%), 0.4 mm (0.8%) for winter. The biases (volume errors) are 10.3 mm (15.8%), 8.1 mm (12.5%), 15.1 mm (23.2%), and 4.6 mm (7.1%) for MXDI01, and 1.2 mm (16.1%), 1.1 mm (15.2%), 1.3 mm (17.0%), and 0.6 mm (8.2%) for MNDI30. After applying the SPP methods, the volume errors of seasonal dam inflow were –3.5–8.5%. However, the VEs of MXDI01 are 7.1–23.2%, and that of MNDI30 are 8.2–17.0%. It can be concluded that the SPP method can correct the average value of dam inflow while they do not effectively reduce the bias of high and low dam inflow.

Figure 4 shows the results of MXDI01 (a) and MNDI30 (b) estimated by the SWAT model with an observation and climate change scenario. The average of probabilistic density function (PDF) of MXDI01 based on a climate change scenario is similar to the PDF of observation. However, the PDFs of MXDI01 are slightly different according to each RCM and SPP method. The average of PDF of MNDI30 based on the climate change scenario is higher than the PDF of observation at the high exceedance probability (9–16 mm/30 days), whereas the PDF of MNDI30

**Table 1** | Statistical analysis of hydrological models

Hydrological model	CC	RMSE (mm/day)	ME	VE (%)
SWAT	0.89	3.05	0.80	–0.07
VIC	0.83	3.90	0.69	3.31

Correlation coefficient (CC) =  $SS_{os} / \sqrt{SS_o \times SS_s}$ ,  $SS_{os} = \sum (O_i - \bar{O})(S_i - \bar{S})$ ,  $SS_o = \sum (O_i - \bar{O})^2$ ,  $SS_s = \sum (S_i - \bar{S})^2$ .

Root mean square error (RMSE) =  $\sqrt{\sum (O_i - S_i)^2 / n}$ , where  $n$  is a number of data.

Nash–Sutcliffe efficiency (ME) =  $[\sum (O_i - \bar{O})^2 - \sum (O_i - S_i)^2] / \sum (O_i - \bar{O})^2$ .

Percent error in volume (VE) =  $100 \times (\sum S_i - \sum O_i) / \sum O_i$ , where  $O$  is observed flow and  $S$  is simulated flow.

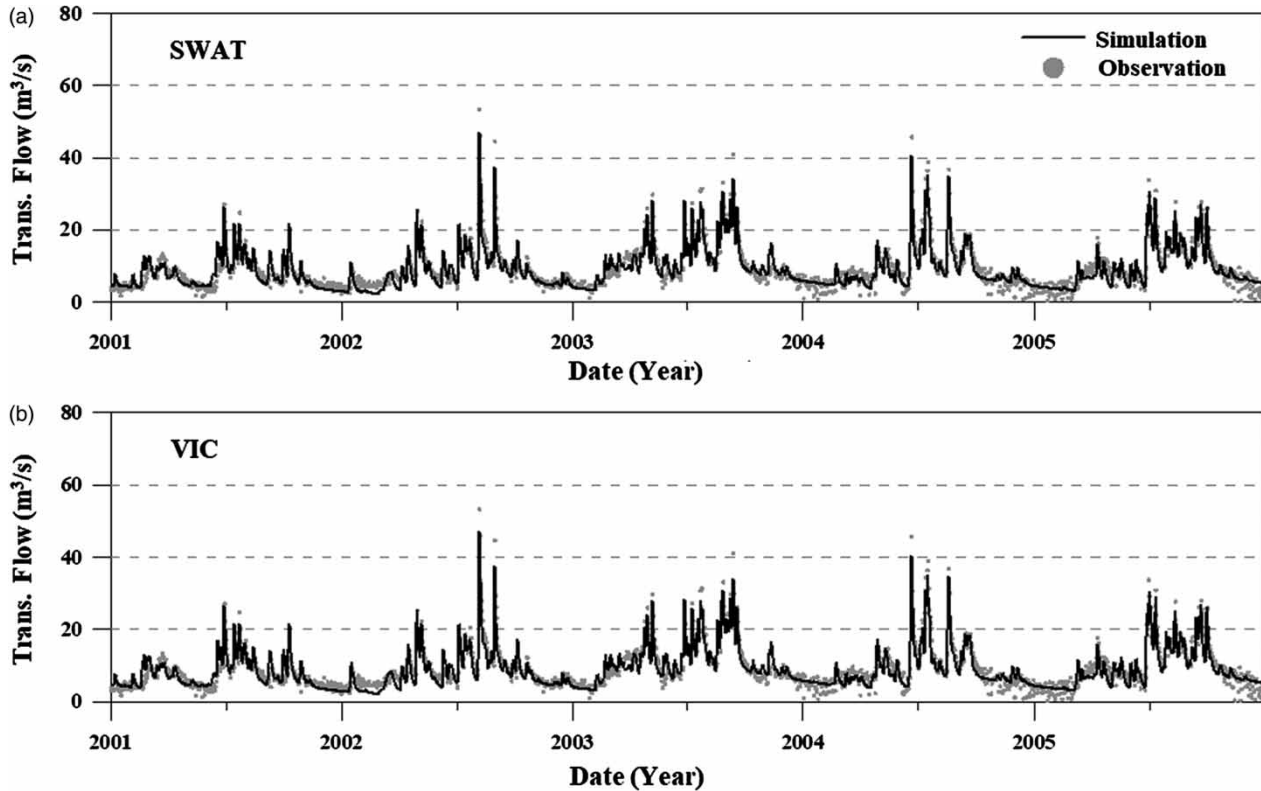


**Figure 3** | Comparison of observed and simulated dam inflow in Chungju Basin (2001–2005). Panels (a) and (b) show the simulation by SWAT and VIC, respectively.

**Table 2** | Comparison of observed and simulated dam inflow (mm)

Type	MXDI01			MNDI30		
	OBS	SWAT	VIC	OBS	SWAT	VIC
Average value	72.6	69.0	61.1	6.5	6.2	8.7
Standard deviation	43.3	39.3	50.4	2.2	2.1	3.2
Maximum	170.8	170.7	223.8	11.3	11.4	18.1
Minimum	19.5	15.0	21.0	3.5	3.3	5.3

is lower than the PDF of observation at the low exceedance probability (3–9 mm/30 days). The PDF of MNDI30 has large differences according to the RCM and SPP methods.

### Future projection

The changes in seasonal dam inflow, MXDI01 and MNDI30 for a future period (2011–2035) relative to the historical

**Table 3** | Biases and volume errors of seasonal runoff, MXDI01 and MNDI30

SPP	Bias (mm)				Volume error (%)			
	LS	VS	QM	SWS	LS	VS	QM	SWS
SPR	11.6	10.9	5.6	4.2	8.5	7.9	4.1	3.1
SUM	24.3	15.7	11.4	9.3	5	3.2	2.3	1.9
AUT	-7.7	-8.4	5.1	-0.5	-3.5	-3.8	2.3	-0.2
WIN	-0.4	-1.8	3	0.4	-0.8	-3.5	5.8	0.8
MXDI01	10.3	8.1	15.1	4.6	15.8	12.5	23.2	7.1
MNDI30	1.19	1.13	1.26	0.61	16.1	15.2	17.0	8.2

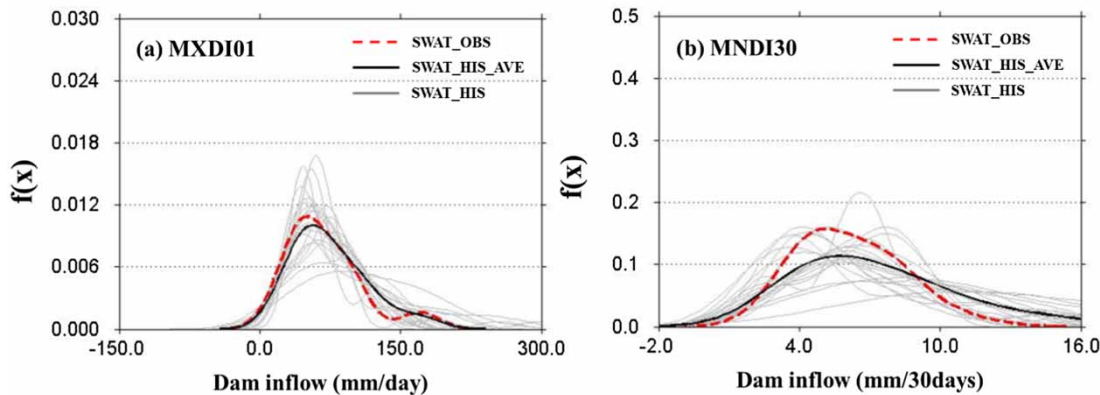


Figure 4 | Comparison in probability density function of MXDI01 (a), MNDI30 (b) for historical period calculated by SWAT model (Lee & Bae 2016).

period (1986–2005) were evaluated. Table 4 shows the future changes in seasonal dam inflow, MXDI01, and MNDI30 according to RCM and HYM. The changes in the dam inflow of spring (March–May), summer (June–August), autumn (September–November), and winter (December–February) are performed. The changes for seasonal dam inflow are 0.1, 58.8, 5.1, and 1.1 mm for the SWAT model and 2.1, 76.1, –8.5, and –2.9 mm for the VIC model for spring, summer, autumn, winter respectively. However, the changes in the summer dam inflow vary (–9.5 mm to +123.9 mm and that of the spring dam inflow vary (–17.2 mm to +19.9 mm) according to the RCM model. Therefore, the RCM effect is larger than the effect of a hydrological model for future projection of the seasonal dam inflow.

In the case of future projection of MXDI01, the average increase is 11.1 mm for the SWAT model and 1.4 mm for the VIC model. The changes of MNDI30 are decreased by about 0.16 mm for SWAT and –0.36 mm for VIC. These results represent that MNDI30 is more sensitive than MXDI01 to the hydrological model. Figure 5 shows the changes in MXDI01 and MNDI30 according to downscaling methods and hydrological models. The changes of MXDI01 do not have consistency according to RCM whereas the changes of MNDI30 are different from the hydrological model. Thus, the RCM and HYM are significant effects for future projection of MXDI01 and MNDI30, respectively. In addition, the change in MXDI01 and MNDI30 of the SWAT model is higher than the VIC model, and the variation of SWAT is higher than VIC. This result shows that

Table 4 | Changes in seasonal dam inflow, MXDI01 and MNDI30 according to RCM and HYM

HYM	RCM	SPR	SUM	AUT	WIN	MXDI01	MNDI30
SWAT	HadGEM3-RA	–9.9	–9.5	–15.9	2.9	4.6	0.57
	RegCM4	6.3	108.4	60.2	2.1	27.1	0.17
	MM5	–17.2	109.1	–17.9	–2.1	8.7	–0.24
	WRF	4.3	75.8	8.4	5.2	18.9	–0.20
	RSM	17.4	10.1	–9.0	–2.4	–2.3	–0.14
	Average	0.1	58.8	5.1	1.1	11.4	0.16
VIC	HadGEM3-RA	–10.5	38.2	–1.8	2.2	–4.6	–0.25
	RegCM4	4.8	77.1	34.2	–3.4	14.0	–0.26
	MM5	–9.9	123.9	–53.3	–5.7	6.7	–0.89
	WRF	6.2	120.9	–12.3	–2.3	–3.0	0.03
	RSM	19.9	20.2	–9.1	–5.2	–6.0	–0.43
	Average	2.1	76.1	–8.5	–2.9	1.4	–0.36



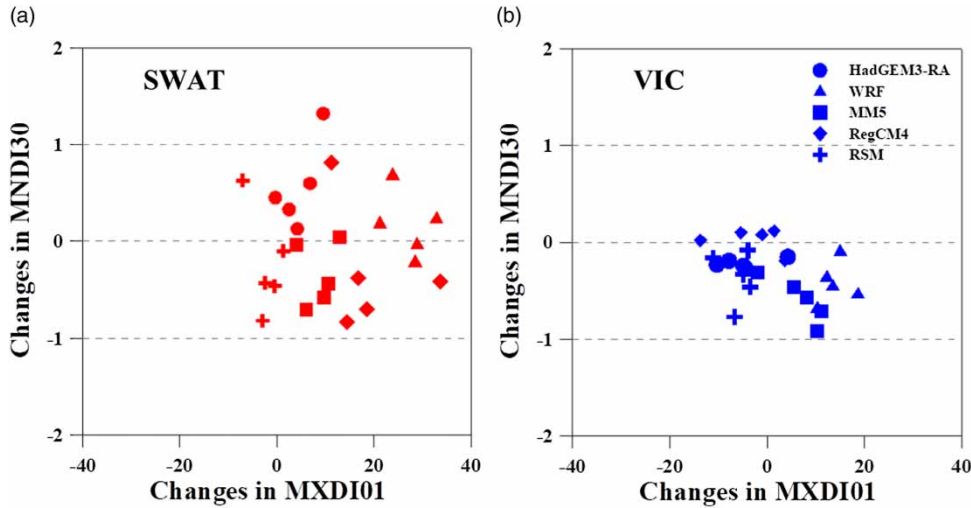


**Figure 5** | Changes in MXDI01 and MNDI30 for future period according to RCMs and SPPs. Panels (a) and (b) show the results of SWAT and VIC, respectively.

the SWAT model is more sensitive to climate change scenario than the VIC model.

### Uncertainty analysis of future projection

In this section, the uncertainty analysis of future projection on dam inflow is performed. Table 5 shows the uncertainty amount and uncertainty contribution for seasonal dam inflow, MXDI01 and MNDI30. The uncertainty amounts (SS) represent the variance of future changes, this study translated uncertainty amounts to standard deviation unit ( $\sqrt{SS}$ ). Thus, uncertainties ( $\sqrt{SS}$ ) of seasonal dam inflow are 5.6, 26.9, 10.4, and 2.9 mm for spring, summer, autumn, and winter, respectively. The contributions of uncertainty from RCM are about 49.6% (spring), 29.3% (summer), 68.9% (autumn), and 13.0% (winter). The RCM

is a dominant source of uncertainty for all seasons except for winter, while the uncertainty contribution of the winter season showed that HYM is the highest source of uncertainty at about 46.5%. The uncertainty contributions of SPP are 3.8–18.7%, the contribution of SPP is smaller than RCM and HYM.

The RCM has the largest sources of uncertainty in MXDI01, which is about 40.7%, while the uncertainty contributions for HYM and SPP are about 35.9 and 2.2%, respectively. However, HYM had the largest sources of uncertainty in MNDI30 (about 41.5%) and the uncertainty contributions for RCM and SPP are about 6.0 and 12.4%, respectively (Figure 6). These variances in the result of high and low flow are caused by the different main factors which have effect for simulating the high and low flow discharge. The high flow is directly affected by the

**Table 5** | Uncertainty analysis of future dam inflow projection

Type	$\sqrt{SS_{total}}$	Uncertainty (SS)					Contribution ( $\eta^2$ )			
		Total	RCM	SPP	HYM	INT	RCM	SPP	HYM	INT
SPR	5.6	30.9	15.3	3.4	5.4	6.8	49.6	10.9	17.5	22.1
SUM	26.9	727.6	212.9	136.3	131.4	247.0	29.3	18.7	18.1	34.0
AUT	10.4	108.5	74.7	4.1	14.7	14.9	68.9	3.8	13.6	13.8
WIN	2.9	8.5	1.1	1.1	3.9	2.4	13.0	12.5	46.5	28.1
MXDI01	4.0	16.3	7.4	0.4	5.2	3.3	40.7	2.2	35.9	21.2
MNDI30	0.7	0.5	0.03	0.06	0.21	0.19	6.0	12.4	41.5	40.1

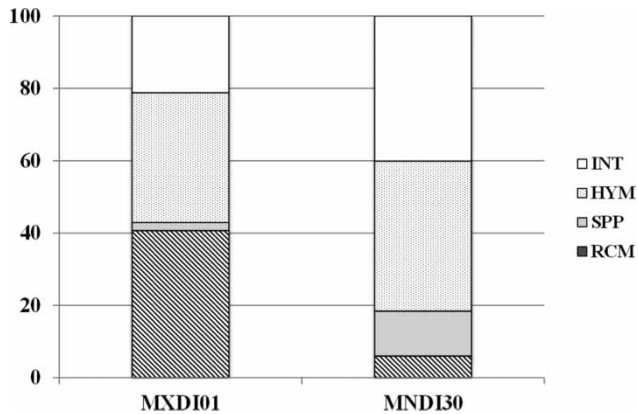


**Figure 6** | Contribution of future projection uncertainty on MXDI01 and MNDI30.

precipitation amount, whereas low flow is affected by soil moisture condition, climate parameters and so on. Therefore, the appropriate ensemble chain will be necessary for the reliable climate change impact assessment.

## SUMMARY AND DISCUSSION

In general, climate change impact assessment on water resources has been performed by using multi-model ensemble scenarios (several GCMs, RCMs and HYMs). All of the impact assessment may face the uncertainty issue. The quantification of the uncertainty is the first step for understanding the uncertainty of future projection. Until now, the climate change uncertainty assessment of previous studies has been performed to compare just uncertainty range (Wilby & Harris 2006; Kay *et al.* 2009; Bae *et al.* 2011; Chen *et al.* 2011; Xu *et al.* 2011; Teng *et al.* 2012; Jung *et al.* 2013). The previous studies also have been focused on the GCM and hydrological model as uncertainty sources of runoff.

This study focused on the uncertainty assessment method for climate change impact assessment and investigated the uncertainty characteristics for high and low flow conditions caused by downscaling methods and hydrological models. The five RCMs (HadGEM3-RA, RegCM4, MM5, WRF, and RSM), five SPPs, and two HYMs were applied to quantify the uncertainty for the future dam inflow in Chungju basin. In the case of future projection of MXDI01, the changes were about 11.4 mm for SWAT, and

1.4 mm for VIC. The changes of MNDI30 were 0.16 mm for SWAT, and  $-0.36$  mm for VIC. The change in MXDI01 and MNDI30 of the SWAT model is higher than the VIC model, and the variation of SWAT is higher than VIC. These results show that the SWAT model is more sensitive to the climate change scenario than the VIC model. The largest source of uncertainty in MXDI01 is from RCM (about 40.7%), while that in MXDI30 is from HYM (about 41.5%). High flow is directly affected by the precipitation amount whereas low flow is affected by soil condition and climate and so on.

Because the future projection based on single RCM and HYM do not have confidence, the appropriate ensemble chains according to target variable will be necessary for reliable climate change impact assessment on water resources. This means that the model chain should consist of the above two hydrological models for low flow projection and the above two RCMs are necessary for high flow projection. The methodology used in this study can be applied to analyze the changes in the total uncertainty according to the specific RCM, SPP, and HYM models. It is also expected that total uncertainty can be reduced based on this approach.

## ACKNOWLEDGEMENTS

This research was supported by the Korea Agency for Infrastructure Technology Advancement (KAIA) grant funded by the Ministry of Land, Infrastructure, and Transport (Grant 18AWMP-B083066-05) and National Research Foundation of Korea (NRF) grant funded by the Korean Government (MSIP) (no. 2011-0030040).

## REFERENCES

- Arnold, J. G., Allen, P. M. & Bemhardt, G. 1993 *A comprehensive surface-groundwater flow model*. *J. Hydrol.* **142**, 47–69.
- Bae, D. H., Jung, I. W. & Chang, H. 2008 *Potential changes in Korean water resources estimated by high-resolution climate simulation*. *Clim. Res.* **35**, 213–226.
- Bae, D. H., Jung, I. W. & Lettenmaier, D. P. 2011 *Hydrologic uncertainties in climate change from IPCC AR4 GCM simulations of the Chungju basin, Korea*. *J. Hydrol.* **401**, 90–105.

- Bae, D. H., Sohn, K. H. & So, J. M. 2017 Utilization of the Bayesian method to improve hydrological drought prediction accuracy. *Water Resour. Manage.* **31**, 3527–3541.
- Baek, H. J., Lee, J., Lee, H. S., Hyun, Y. K., Cho, C. H., Kwon, W. T., Marzin, C., Gan, S. Y. & Kim, M. J. 2013 Climate change in the 21st century simulated by HadGEM2-AO under representative concentration pathways. *Asia Pac. J. Atmos. Sci.* **49**, 603–618.
- Bastola, S., Murphy, C. & Fealy, R. 2012 Generating probabilistic estimates of hydrological response for Irish catchments using a weather generator and probabilistic climate change scenarios. *Hydrol. Process.* **26**, 2307–2321.
- Bosshard, T., Carambia, M., Goergen, K., Kotlarski, S., Krahe, P., Zappa, M. & Schar, C. 2013 Quantifying uncertainty sources in an ensemble of hydrological climate-impact projections. *Water Resour. Res.* **49**, 1523–1536.
- Chen, J., Brissette, F. P. & Leconte, R. 2011 Uncertainty of downscaling method in quantifying the impact of climate change on hydrology. *J. Hydrol.* **401**, 190–202.
- Deque, M., Rowell, D. P., Luthi, D., Giorgi, F., Christensen, J. H., Rockel, B., Jacob, D., Kjellstrom, E., Castro, M. & van den Hurk, B. 2007 An intercomparison of regional climate simulations for Europe: assessing uncertainties in model projections. *Clim. Change* **81**, 53–70.
- Harvey, H., Hall, J. & Peppe, R. 2012 Computational decision analysis for flood risk management in an uncertain future. *J. Hydroinform.* **14** (3), 537–561.
- IPCC 2013 *Climate Change 2013 The Physical Scientific Basis, IPCC Contribution of Working Group I to the Fifth Assessment Report of the Intergovernmental Panel on Climate Change*. Cambridge University Press, Cambridge.
- Jung, I. W., Bae, D. H. & Lee, B. J. 2013 Possible change in Korean streamflow seasonality based on multi-model climate projections. *Hydrol. Process.* **27** (7), 1033–1045.
- Kay, A. L., Davies, H. N., Bell, V. A. & Jones, R. G. 2009 Comparison of uncertainty sources for climate change impacts: flood frequency in England. *Clim. Change* **92**, 41–63.
- Lee, M. H. & Bae, D. H. 2013 Evaluation of hybrid downscaling method combined regional climate model with Step-wise Scaling method. *J. Korea Water Resour. Assoc.* **46**, 585–596.
- Lee, M. H. & Bae, D. H. 2015 Climate change impact assessment on green and blue water over Asian monsoon region. *Water Resour. Manage.* **28** (7), 2407–2427.
- Lee, M. H. & Bae, D. H. 2016 Uncertainty assessment of future high and low flow projections according to climate downscaling and hydrological models. *Proc. Eng.* **154**, 617–623.
- Liang, X., Lettenmainer, D. P., Wood, E. F. & Burges, S. J. 1994 A simple hydrologically based model of land surface water and energy fluxes for General Circulation Models. *J. Geophys. Res.* **99**, 14415–14428.
- Mani, A. & Tsai, F. T. C. 2017 Ensemble averaging methods for quantifying uncertainty sources in modeling climate change impact on runoff projection. *J. Hydrol. Eng.* **22**, 04016067.
- Park, C., Min, S. & Lee, D. 2016 Evaluation of multiple regional climate models for summer climate extremes over East Asia. *Clim. Dynam.* **46** (7), 2469–2486.
- Raghavan, S. V., Tue, V. M. & Liang, S. Y. 2014 Impact of climate change on future stream flow in the Dakbla river basin. *J. Hydroinform.* **16** (1), 231–244.
- Steinschneider, S., Polebitski, A., Brown, C. & Letcher, B. H. 2012 Toward a statistical framework to quantify the uncertainties of hydrologic response under climate change. *Water Resour. Res.* **48**, W11525.
- Suh, M. S., Oh, S. G., Lee, D. K., Cha, D. H., Choi, S. J., Jin, C. S. & Hong, S. Y. 2012 Development of new ensemble methods based on the performance skills of regional climate models over South Korea. *J. Clim.* **25**, 7067–7082.
- Teng, J., Vaze, J., Chiew, F. H., Wang, B. & Perraud, J. M. 2012 Estimating the relative uncertainties sourced from GCMs and hydrological models in modeling climate change impact on runoff. *J. Hydrometeorol.* **13** (1), 122–139.
- Teutschbein, C. & Seibert, J. 2012 Bias correction of regional climate model simulations for hydrological climate-change impact studies: review and evaluation of different methods. *J. Hydrol.* **456**, 12–29.
- Vojinovic, Z., Sahlu, S., Torres, A. S., Seyoum, S. D., Anvarifar, F., Matungulu, H., Barreto, W., Savic, D. & Kapelan, Z. 2014 Multi-objective rehabilitation of urban drainage systems under uncertainties. *J. Hydroinform.* **16** (5), 1044–1061.
- Wilby, R. L. & Harris, I. 2006 A framework for assessing uncertainties in climate change impacts: low-flow scenarios for the River Thames, U.K. *Water Resour. Res.* **42**, W02419.
- Xu, H., Taylor, R. G. & Xu, Y. 2011 Quantifying uncertainty in the impacts of climate change on river discharge in sub-catchments of the Yangtze and Yellow River basin, China. *Hydrol. Earth Syst. Sci.* **15**, 333–344.
- Yu, P. S., Yang, T. C., Kuo, C. M. & Chen, S. T. 2014 Development of an integrated computational tool to assess climate change impacts on water supply-demand and flood inundation. *J. Hydroinform.* **16** (3), 710–730.
- Zhang, C., Zhu, X. P., Fu, G. T., Zhou, H. C. & Wang, H. 2014 The impacts of climate change on water diversion strategies for a water deficit reservoir. *J. Hydroinform.* **16** (4), 872–889.

First received 10 October 2017; accepted in revised form 22 February 2018. Available online 29 March 2018